Proceedings of Ninth World Conference on Earthquake Engineering
August 2-9, 1988, Tokyo-Kyoto, JAPAN (Vol.IV)

6-7-1

CYCLIC BEHAVIOR OF STEEL AND COMPOSITE JOINTS WITH PANEL ZONE DEFORMATION

Le-Wu LU[1], Shiunn-Jang WANG[1] and Seung-Joon LEE[2]

[1]Department of Civil Engineering, Lehigh University,
Bethlehem, Pennsylvania, U.S.A.
[2]Department of Architecture, Ajou University,
Suweon, Korea

SUMMARY

The behavior of steel and composite beam-to-column joints with panel zone deformation has been studied both analytically and experimentally. The main objectives are to evaluate the load-deformation characteristics, and to develop analytical models to predict their behavior. This paper presents the models developed and the close correlations between analytical predictions and test results. The hysteretic models are based on the results of extensive nonlinear finite element and a cyclic plasticity model for steel.

INTRODUCTION

In seismic design of moment-resistant frames, it is often necessary to use girders that may be considerably larger than those required to satisfy the allowable-stress criteria in order to control drift. At the code seismic force level, the stresses in these girders may therefore be substantially less than the allowable values. However, when such a frame is subjected to a major earthquake and is assumed to remain elastic, the lateral forces generated could be several times greater than the code forces. Inelastic action must therefore take place in the highly stressed regions of the structure. One such region is the beam-to-column joints. The current design practices permit inelastic action to develop in the panel zone of the joints and this action may be utilized to dissipate part of the energy input. The amount of inelastic deformation required of the joints is related to the characteristics of the earthquake ground motion and the properties of the frame. A complete inelastic seismic response analysis is necessary in order to determine the inelastic joint deformation and to evaluate overall performance of the structure. However, before such an analysis can be performed, the behavior of joints with panel zone deformation must be well understood and properly represented by analytical models.

Two series of beam-to-column assemblages have been tested under repeated loads (1, 2) and analytical study of the cyclic behavior of joints have been carried out (2, 3). As the results of the study, analytical models have been proposed for predicting the behavior of steel and composite joints.

MODEL FOR STEEL JOINTS

Virgin Behavior For joint under monotonic loading, a trilinear model is

proposed (Fig. 1). The joint behavior is divided into three ranges:

Elastic range: In this range, it is assumed that the shear force is taken by panel only and shear stress is uniformly distributed within the panel. The shear force-distortion relationship can be expressed by the following formula:

$$\gamma = \frac{V}{(d_c - 2t_{cf})t_{cw}G} \tag{1}$$

$$V = \frac{\Delta M}{(1-\rho)(d_b - t_{bf})} \tag{2}$$

where ΔM is the moment applied to the joint, d_c, the depth of the column, t_{cf}, the thickness of the column flange, t_{cw}, the thickness of the column web, d_b the depth of the beam, t_{bf}, the thickness of the beam flange, G, the shear modulus of steel and $\rho = \Delta M/h_c$ (h_c is the height of the column).

Plastic range: After panel yields, column flange is the major element in resisting shear force. From limit analysis, the column flange contribution to joint shear strength can be computed as $4M_{pcf}$, where M_{pcf} is the plastic moment of the column flange. In terms of shear force, the contribution of column flange can be written as:

$$\Delta V = \frac{4M_{pcf}}{(1-\rho)(d_b - t_{bf})} \tag{3}$$

Also, from finite element analysis, the average rotation when panel reaches strain hardening is $3.5\gamma_y$. Therefore, this range starts from (V_y, γ_y) to ($V_y + \Delta V$, $3.5\gamma_y$) on the load-deformation curve.

Strain-hardening range: After the panel reaches strain hardening, the joint stiffness is a function of G_{st}, the strain hardening shear modulus of the material.

Cyclic Behavior The following observations made from analytical and experimental studies are used in developing the model:

1. Before the joint rotation reaches $2\gamma_y$, the joint behavior can be predicted by a virgin curve associated with kinematic hardening rule.
2. The cyclic joint behavior is mostly controlled by the shear modulus for reversals after the panel is fully yielded, the joint behavior can be approximately divided into four constant stiffness ranges just as in the material model.
3. The contribution of column flange can be included in the model by using $V_y + 2M_{pcf}/(d_b - t_{bf})$ and the corresponding elastic rotation as the normalizing factors.
4. For large plastic rotation, shear strain distributed uniformly within the panel and the value of joint rotation is close to the value of shear strain in the panel. Therefore, the material property of the panel can be predicted by using joint rotation and the force-rotation relationship of the joint can be obtained by assuming all the shear is taken by the panel only.
5. The joint tends to work its way to the cyclic steady curve at any time of the cyclic loading history.
6. In each cycle, a positive and a negative bound exist whose positions are a function of the past loading history. The same rules for updating bounding lines in cyclic material model (3) apply to the model for cyclic joint behavior.

In the model developed, which is shown in Fig. 2, any cycle after the joint rotation exceeds $2\gamma_n$ is represented by four straight lines and the bounding lines

are updated according to the force level of the last excursion. The load-deformation relationship of the joint is expressed as the relationship between normalized shear force and rotation. V/V_n and γ/γ_n. V_n and γ_n are defined as:

$$V_n = V_y + \frac{2M_{pcf}}{d_b - t_{bf}} \tag{4}$$

$$\gamma_n = \frac{V_n}{(d_c - 2t_{cf})t_{cw}G} \tag{5}$$

After the joint rotation exceeds $2\gamma_n$, positive bound and negative bound are established to pass (V_{max}/V_n, 0) and ($-V_{max}/V_n$,0) respectively, as shown in Fig. 3, where V_{max} is the maximum shear the joint experienced before reversal. Each branch of the hysteresis loop is represented by four straight lines. The slope of these four lines can be computed using the corresponding shear modulus in the material model. Before the shear reaches zero, unloading is assumed to follow the elastic slope. After the load changes sign, two lines are used to describe the path before the path meets with the bound. The range of line BC in Fig. 2 is defined as $0.65V_{bound}$ where V_{bound} is the corresponding shear load of the point at which the bound in the direction of the current loading meets the shear load axis.

If reversal occurs in the elastic range, no update of the bound is necessary. The path in the next excursion will be elastic until the original force-deformation path in this direction is reached and the deformation is assumed to continue along this curve as if no interruption has taken place. After every reversal, except in the elastic range, the subsequent shear load bound is updated according to the response of the last excursion. The rules for updating the bounds are described in detail in Ref. 3.

Comparison with Experimental Results In Fig. 4, the results from a 1981 Lehigh test are plotted against the predictions made by the proposed model. The model underestimates slightly the joint strength in all the cycles. However, the match is satisfactory considering the simplicity of the model and the complexity of the problem.

MODEL FOR COMPOSITE JOINTS

The model is a trilinear approximation of the true inelastic deformation characteristics. The cyclic joint behavior characteristics observed in the test and the assumptions made for the modelling are summarized below:

1. Exterior joint panel zone exhibited non-symmetric response due to the effect of composite slab, but hysteresis loops of interior panel zone are assumed to be symmetric shape even if its actual behavior depends on the moments at both ends.
2. Beam moments are replaced by forces, Q, at the column face, as shown in Fig. 5, and the effect of composite slab is simulated by the increase of beam depth to D_b+.
3. Post-yield deformation of panel zone is limited to the area bounded by the flange of steel beams and columns (shaded area in Fig. 5).
4. Under cyclic loading, the panel zone exhibits strain-hardening behavior between isotropic hardening and kinematic hardening.

Skeleton Curve A trilinear model is proposed which divide the joint behavior into three stages:

Elastic Range: Only the elastic stiffness of the panel zone for resisting the shear load is considered in this range.

Plastic range: The extra strength beyond general yielding is provided by column flanges and strain-hardening of panel zone. The total shear increase is:

$$\Delta V = \left[\frac{12EI_{cf}}{d_b^2} + \frac{2EI_{cf}}{t_{cf}\, d_b} + t_{cw}(d_c - 2t_{cf})G_{st} \right] \Delta\gamma_p \qquad (6)$$

where I_{cf} is the moment of inertia of the column flange and $\Delta\gamma_p$ is the panel zone plastic distortion.

Strain-Hardening Range: The post-yield or plastic stiffness is assumed to remain constant until the boundary frame yields and forms a mechanism. After that, only strain hardening of the panel is considered.

The response curve for exterior joint under positive moment is different than that under negative moment (Fig. 6). For the interior joint, the curve is symmetrical. Figs. 7 and 8 show comparison of the analytical and experimental curves. The overall predictions provided by the proposed model appears to be good.

Hysteresis Behavior Based on the experimental and the finite element analysis results, the following rules for hysteresis behavior are proposed (Fig. 6):

1. Moment-shear distortion relationship of panel zone is elastic up to the general yield point in each direction.
2. Once the general yield strength is exceeded, loading proceeds on the post-elastic stiffness, K_{inel}.
3. Once the load passes the plastic strength, strain hardening stiffness is assumed.
4. Unloading from the 2^{nd} and 3^{rd} slopes is parallel to the elastic stiffness, and extended to the reloading curve up to point B or C which is the mid-point between the isotropic and kinematic hardening yield surfaces. For simplicity, points B and C are fixed at 55% and 65%, respectively, of the previously reached maximum moments.
5. For an exterior joint under negative moment, reloading after rule 4 is parallel to the negative post-elastic stiffness, K_{inel}, and discontinued at the plastic moment, where the strain-hardening stiffness follows.
6. For an exterior joint under positive moment and for interior joint, reloading after rule 4 is toward the previous maximum point in that direction.
7. If the direction of moment changes while closing the crack, an unloading slope equal to the elastic slope is used.

SUMMARY

Two analytical models capable of describing the cyclic behavior of steel and composite joints have been presented. Predictions made by the models show good agreement with test results. The models have been incorporated in the nonlinear dynamic analysis of steel buildings with or without composite slab (2, 3).

REFERENCES

1. Slutter, R. G., "Tests of Panel Zone Behavior in Beam-Column Connection" Fritz Engineering Laboratory Report No. 200.81.403.1, Lehigh University, Bethlehem, PA, 1981.

2. Lee, S. J., "Seismic Behavior of Steel Building Structures with Composite Slabs", Ph.D. Dissertation, Lehigh University, 1987.
3. Wang, S. J. "Seismic Response of Frames with Significant Inelastic Joint Deformation", Ph.D. Dissertation, Lehigh University, 1988.

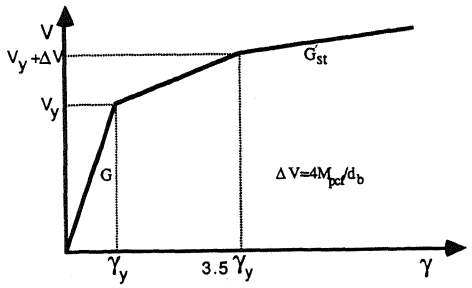

Fig. 1. Schematic showing of proposed model for monotonic joint behavior.

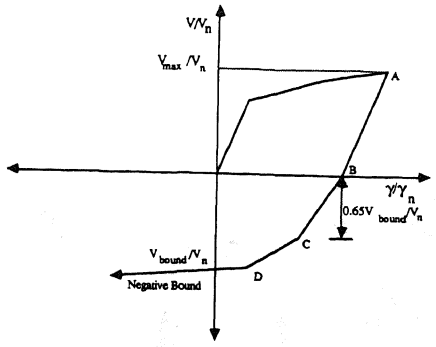

Fig. 2. Schematic showing of proposed model for cyclic joint behavior.

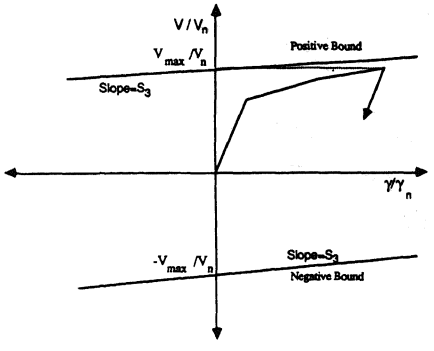

Fig. 3. Initial establishment of bounds.

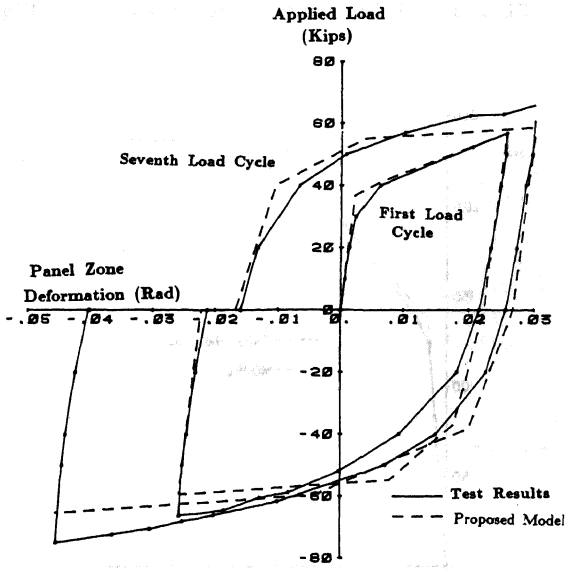

Fig. 4. Comparison of proposed model and 1981 Lehigh test.

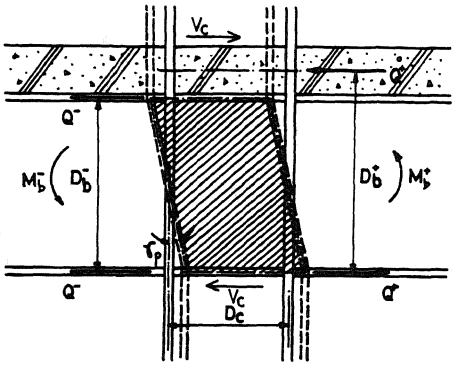

Fig. 5. Joint panel zone model.

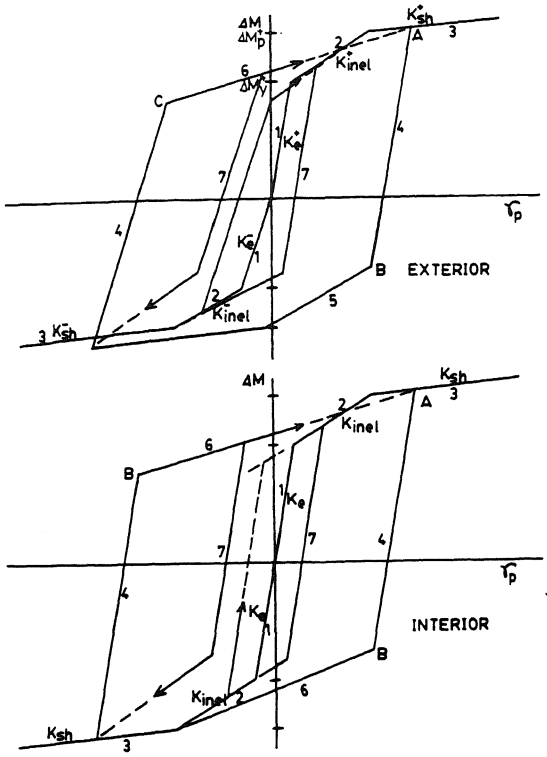

Fig. 6. Hysteresis rules of composite beam-to-column joint.

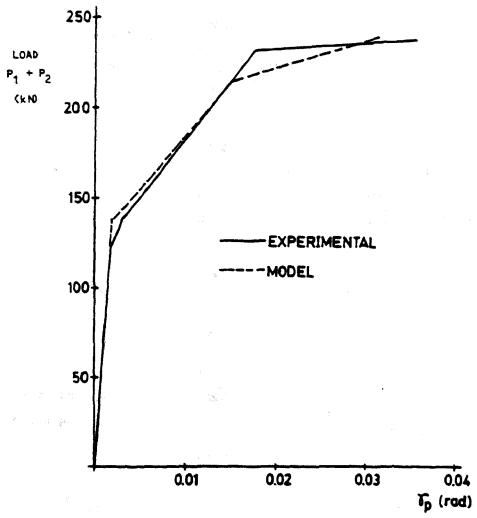

Fig. 7. Experimental curve vs. analytical model of an exterior composite joint.

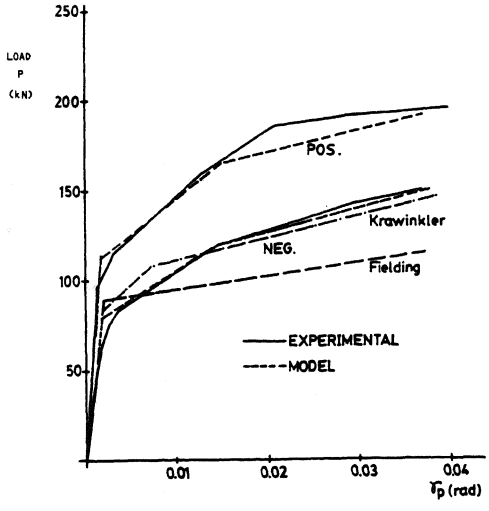

Fig. 8. Experimental cruve vs. analytical model of an interior composite joint.